Supplementary Information (SI) for ChemComm.
This journal is © The Royal Society of Chemistry 2026

Experimental Details

Preparation of Cu-SSZ-13

As-synthesized SSZ-13 was prepared following a previously reported method.[1] This material was then converted to H-SSZ-13 via ammonium ion exchange followed by calcination. Finally, copper ion exchange was performed to obtain the Cu-SSZ-13 catalyst.

SSZ-13 zeolite synthesis:

The as-synthesized SSZ-13 sample was prepared by hydrothermal synthesis using N, N, N-trimethyl-1-adamantammonium hydroxide (TMAdaOH) as the structure-directing agent (SDA), colloidal silica and aluminum hydroxide as the Si and Al sources, and seed crystals. The synthesis was conducted in the presence of NaOH and KOH. The product was washed, dried, and calcined to remove the SDA.

Proton ion-exchange:

The calcined SSZ-13 was subjected to ion exchange twice using 1.2 M NH_4NO_3 at 80°C for 2 h. The resulting material was thoroughly washed, dried, and subsequently calcined at 550°C for 3 h to obtain the H-form zeolite (H-SSZ-13).

Copper ion exchange:

The H-SSZ-13 sample was treated twice with a 0.05 M Cu $(CH3COO)_2 \cdot H_2O$ solution at 50°C for 2 h to carry out ion exchange. The sample was thoroughly washed and dried and then calcined at 500°C for 2 h to obtain the final Cu-SSZ-13 sample.

Preparation of Cu-SSZ-39

SSZ-39 zeolite synthesis:

An aqueous solution of N, N-dimethyl-3,5-dimethylpiperidinium hydroxide was mixed with water and amorphous $Al(OH)_3$ and stirred (300 rpm, 15 min) at room temperature. Snowtex-40 (SiO_2, 40 wt%) was added to the resulting solution to prepare Slurry A. An aqueous NaOH solution (Solution B) was added dropwise to Slurry A to form a synthesis gel. The gel was aged at 80°C for 4 h under stirring (300 rpm). Finally, uncalcined CHA-type zeolite (SiO_2/Al_2O_3 = 23) seeds were added to the gel, and the mixture was stirred for an additional 30 min at room temperature to obtain a precursor gel. The molar composition of the precursor gel was 1.0 SiO_2:0.071 Al_2O_3:0.35 NaOH:17.5 H_2O:0.1 OSDA. The precursor gel was loaded into a stirred-tank reactor and subjected to hydrothermal synthesis at 180°C and 60 rpm for 25.5 h. The product was filtered, recovered, and dried

to obtain a powder. X-ray diffraction (XRD) analysis confirmed that the obtained crystals were an AEI-type zeolite. X-ray fluorescence (XRF) analysis showed that the SiO_2/Al_2O_3 molar ratio of the obtained zeolite was 10.3. To remove organic materials from the zeolite, the synthesized zeolite powder was calcined at 600°C under an air flow for 6 h.

Proton ion exchange:

The calcined zeolite was dispersed in a 2.7 M NH_4NO_3 aqueous solution to remove Na^+ ions, yielding a 14 wt% slurry. The slurry was stirred at 80°C for 1 h to carry out ion exchange and then subjected to filtration and washing with deionized water three times. The entire ion exchange and washing procedure was repeated. The resulting zeolite powder was dried at 100°C for 12 h to obtain an NH_4-SSZ-39 zeolite. Finally, the NH_4-AEI zeolite was calcined at 500°C under an air flow for 2 h to remove NH_3, yielding H-SSZ-39.

Copper ion exchange:

Copper acetate ($Cu(OAc)_2 \cdot H_2O$) was dissolved in water to prepare a 0.05 M copper acetate (II) aqueous solution. This copper acetate (II) solution was mixed with H-AEI zeolite powder in a 10:1 weight ratio to prepare a dispersion. The dispersion was stirred at room temperature for 2 h to perform ion exchange. The zeolite was recovered by filtration and washed three times with deionized water. The obtained zeolite powder was subjected to the same ion exchange process and then dried at 100°C for 12 h to yield the Cu-loaded AEI zeolite. An XRF analysis showed that the Cu-loaded AEI zeolite had a Cu/Al molar ratio of 0.29 and a Cu content of 4.7 wt%.

Hydrothermal aging (HTA)

The hydrothermal stability of the samples was evaluated by aging in an airflow containing 10 vol.% H_2O at 800 °C for 5 h. The gas hourly space velocity (GHSV) was set to 3000 h^{-1}.

NH_3-SCR activity test

The catalytic activity of the samples was tested in a fixed-bed quartz flow reactor at atmospheric pressure. Catalyst pellets (particle size: 600–1000 μm) were loaded into the reactor, and the GHSV was set to 2.0×10^5 h^{-1}. The inlet feed contained 350 ppm nitrogen oxides (NO_x), 385 ppm NH_3, 14 vol.% O_2, and 5 vol.% H_2O, with N_2 as the balance gas. The NO_x conversion was calculated as follows:

$$NO_x \text{ conversion} = \left(1 - \frac{[NO_x]out}{[NO_x]in}\right) \times 100\ (\%)$$

Composition analysis

The SiO_2/Al_2O_3 and Cu/Al ratios in the zeolite framework were determined using the following method. A standard zeolite sample was dissolved through heat treatment in an alkaline aqueous solution and a hydrofluoric acid solution. The SiO_2/Al_2O_3 and Cu/Al ratios were then measured using inductively coupled plasma optical emission spectroscopy (iCAP 7600, Thermo Fisher Scientific). A standard sample was analyzed using XRF (Supermini 200, Rigaku) to generate calibration curves relating the fluorescence X-ray intensity of the target elements to their atomic concentrations. The calibration curves were used in conjunction with XRF to determine the SiO_2/Al_2O_3 and Cu/Al ratios of the zeolite sample under investigation.

XRD analysis

Powder XRD patterns were recorded on a diffractometer (D2 Phaser, Bruker AXS) using Cu Kα radiation (λ = 1.5406 Å, 30 kV, 10 mA). Data were collected over a 2θ range of 3–50° using a step size of 0.02°.

Scanning electron microscopy with energy–dispersive X-ray spectroscopy (SEM–EDS) analysis

Powdered Cu-SSZ-13 or Cu-SSZ-39 samples were dry-dispersed (without using a solvent) onto a Mo TEM grid (EM Japan Co. Ltd.). A SEM–EDS analysis was performed using a scanning electron microscope (SU-5000, Hitachi High-Tech corp.) equipped with an EDS system (Flash FlatQUAD, Bruker Corporation). The accelerating voltage was set to 4 kV.

Transmission electron microscopy (TEM) and electron ptychography observations

Pretreatment before observation:

The powder samples were deposited onto carbon-coated copper TEM grids (EM Japan) by dry dispersion (for the fresh H-SSZ-13 and Cu-SSZ-13 samples) or by dispersion in ethanol (for the aged Cu-SSZ-13 sample and the Cu-SSZ-39 sample before and after aging). Ethanol was selected as the dispersion solvent to ensure that the fine particles could be effectively dispersed on the TEM grid. The grids were then heated on a hot plate at 200 °C for 20 min and subsequently cooled to 25 °C under ambient conditions. The cooled grids were immediately loaded into a double-tilt TEM holder (JEOL) under ambient conditions.

Observation conditions:

The samples on the TEM grids were observed using an aberration-corrected transmission electron microscope (JEM-ARM200F, JEOL) equipped with a pixelated detector (4DCanvas, JEOL) at an accelerating voltage of 200 kV. During ptychography, diffraction patterns were acquired at each probe point under the following conditions. The convergence angle was set to 20.8 mrad, and the probe current ranged from 0.06 to 0.18 pA (corresponding to 49–150 electrons). The real-space resolution was set to 512 × 512 pixels. The pixel size was set to 0.019 nm. Diffraction patterns were initially acquired at a resolution of 264 × 66 pixels and subsequently binned to 66 × 66 pixels during postprocessing. The frame rate was fixed at 7500 fps. The camera length was adjusted such that the transmitted beam occupied approximately 80% of the detector area, corresponding to an angular resolution of 0.5 mrad per pixel. Ptychographic reconstruction was performed using the Wigner distribution deconvolution method[2] and an in-house Python code.[1] Postaberration estimation and correction were performed using a method proposed by Yang et al.[3]

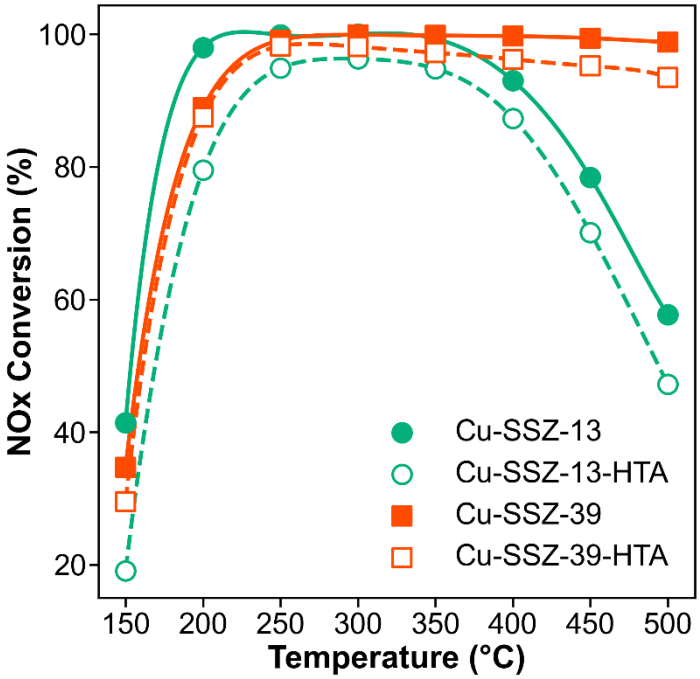

Figure S1

NO_x conversion of fresh and hydrothermally aged (800 °C, 5 h) Cu-SSZ-13 and Cu-SSZ-39 during the standard ammonia selective catalytic reduction (NH_3-SCR) reaction.

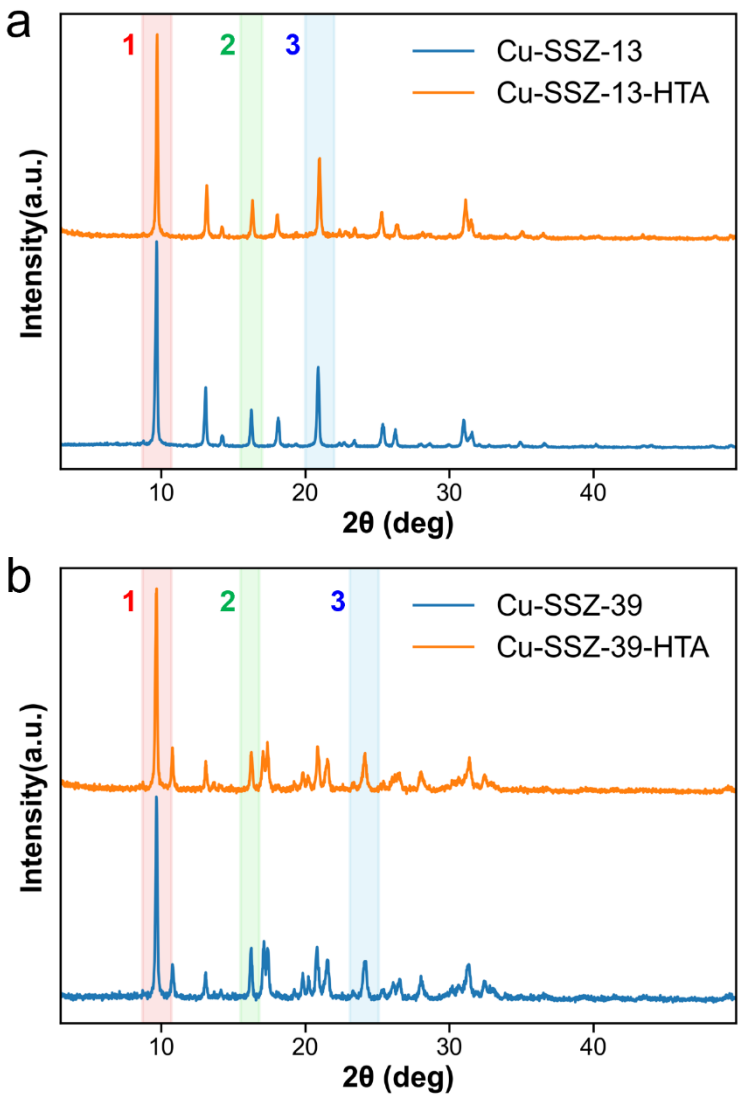

Figure S2

X-ray diffraction (XRD) patterns of (a) Cu-SSZ-13 and (b) Cu-SSZ-39 obtained before and after hydrothermal aging (HTA). All the patterns are normalized and vertically offset to prevent overlap. The peaks in the regions labeled 1–3 were used to calculate the full width at half maximum (FWHM). The calculated FWHMs for each peak are shown in Table S1.

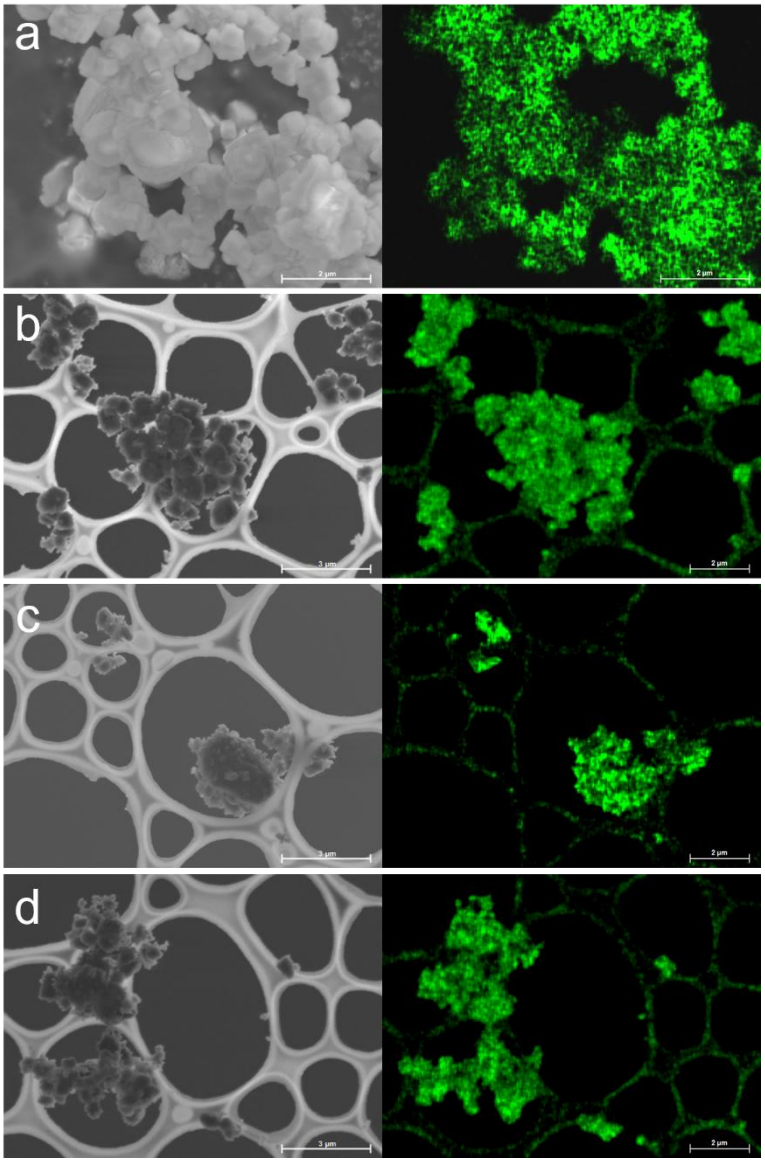

Figure S3

Scanning electron microscopy (SEM) images and energy dispersive spectroscopy (EDS) elemental maps (Cu L line) of Cu-SSZ-13 and Cu-SSZ-39 obtained before and after hydrothermal aging (HTA): (a) Cu-SSZ-13, (b) Cu-SSZ-13-HTA, (c) Cu-SSZ-39, and (d) Cu-SSZ-39-HTA.

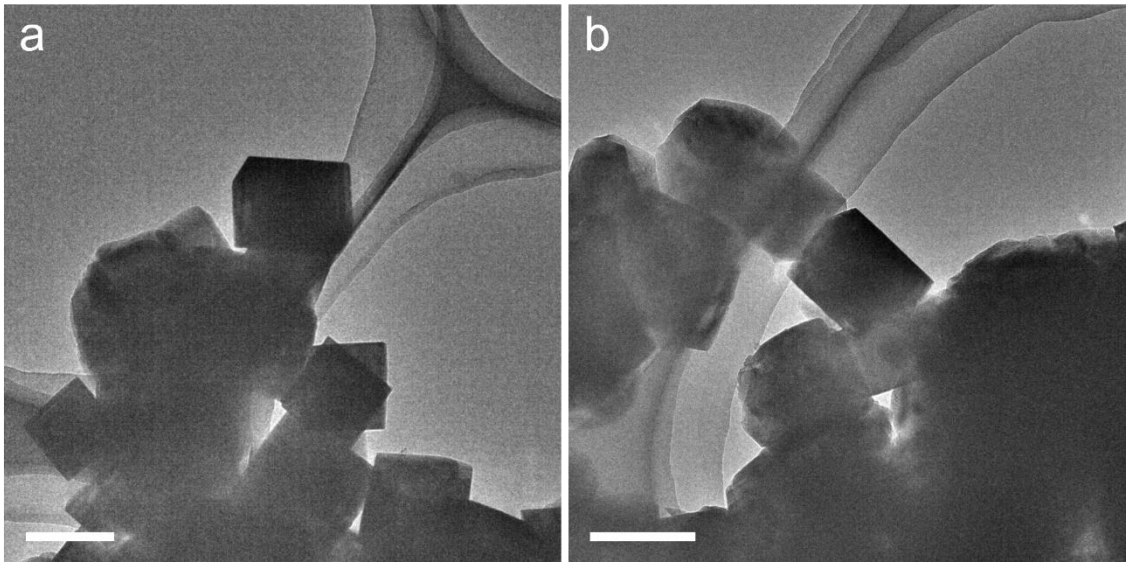

Figure S4

Transmission electron microscopy (TEM) images of (a) Cu-SSZ-13 and (b) Cu-SSZ-13-HTA. Scale bar: 500 nm. HTA: hydrothermal aging.

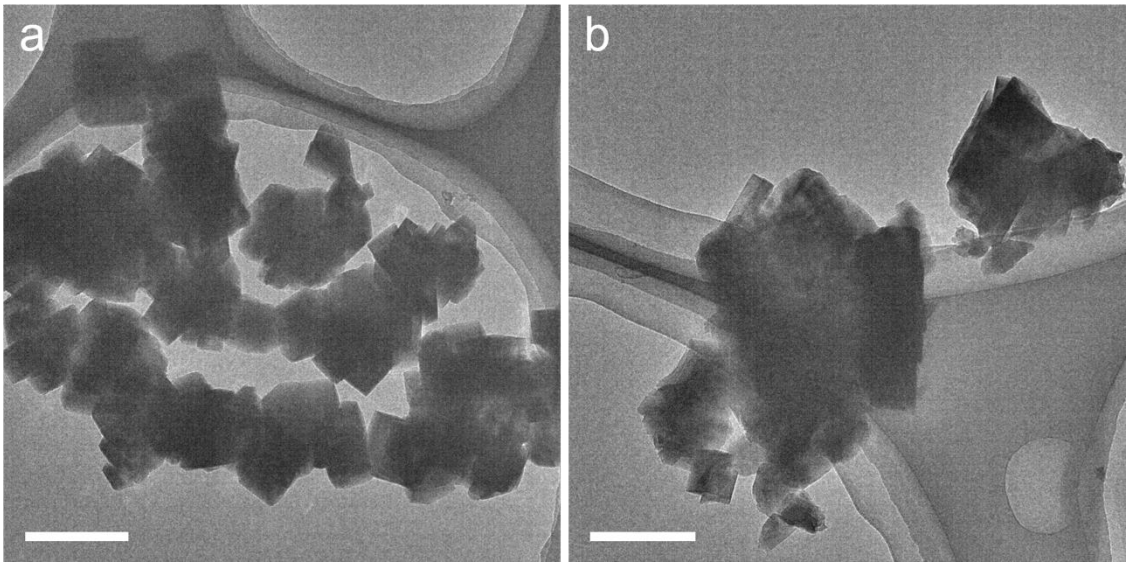

Figure S5

Transmission electron microscopy (TEM) images of (a) Cu-SSZ-39 and (b) Cu-SSZ-39-HTA. Scale bar: 500 nm. HTA: hydrothermal aging.

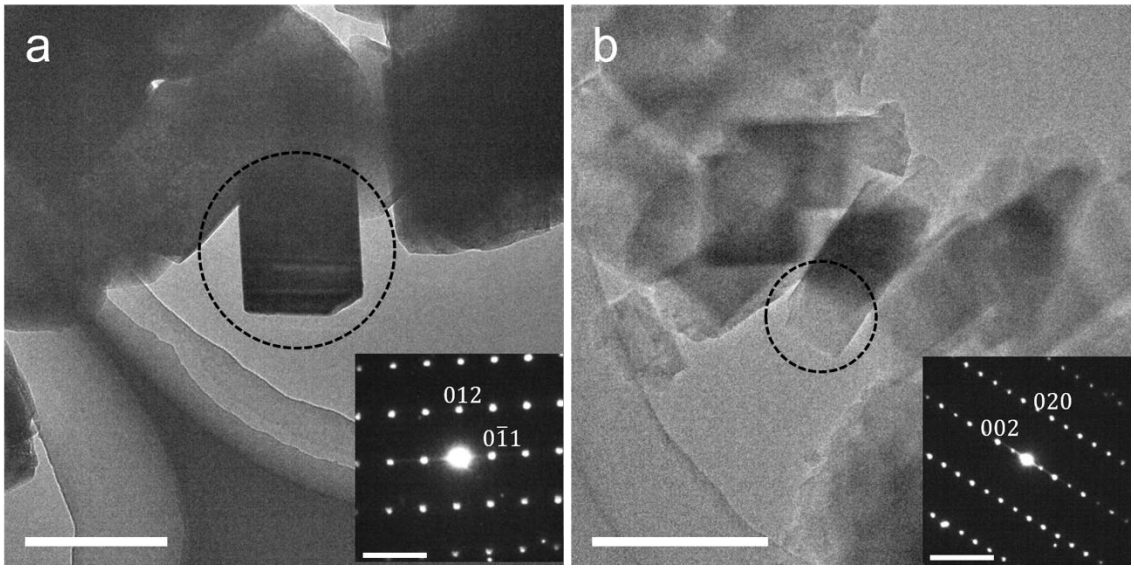

Figure S6

Transmission electron microscopy (TEM) images showing the particle morphology of (a) Cu-SSZ-13-HTA and (b) Cu-SSZ-39-HTA. The insets show selected-area electron diffraction (SAED) patterns acquired for the regions delineated by the dashed circles. The sharp diffraction spots that appear in the SAED patterns of both samples indicate that the zeolites retain their crystalline structures and confirm that the electron beam is aligned along the [100] zone axis of the Cu-SSZ-13/Cu-SSZ-39 particles in the regions within the dashed circles. Scale bars: 500 nm (TEM) and 2 nm^{-1} (SAED). Radii of the dashed circles: 350 nm in (a) and 130 nm in (b). HTA: hydrothermal aging.

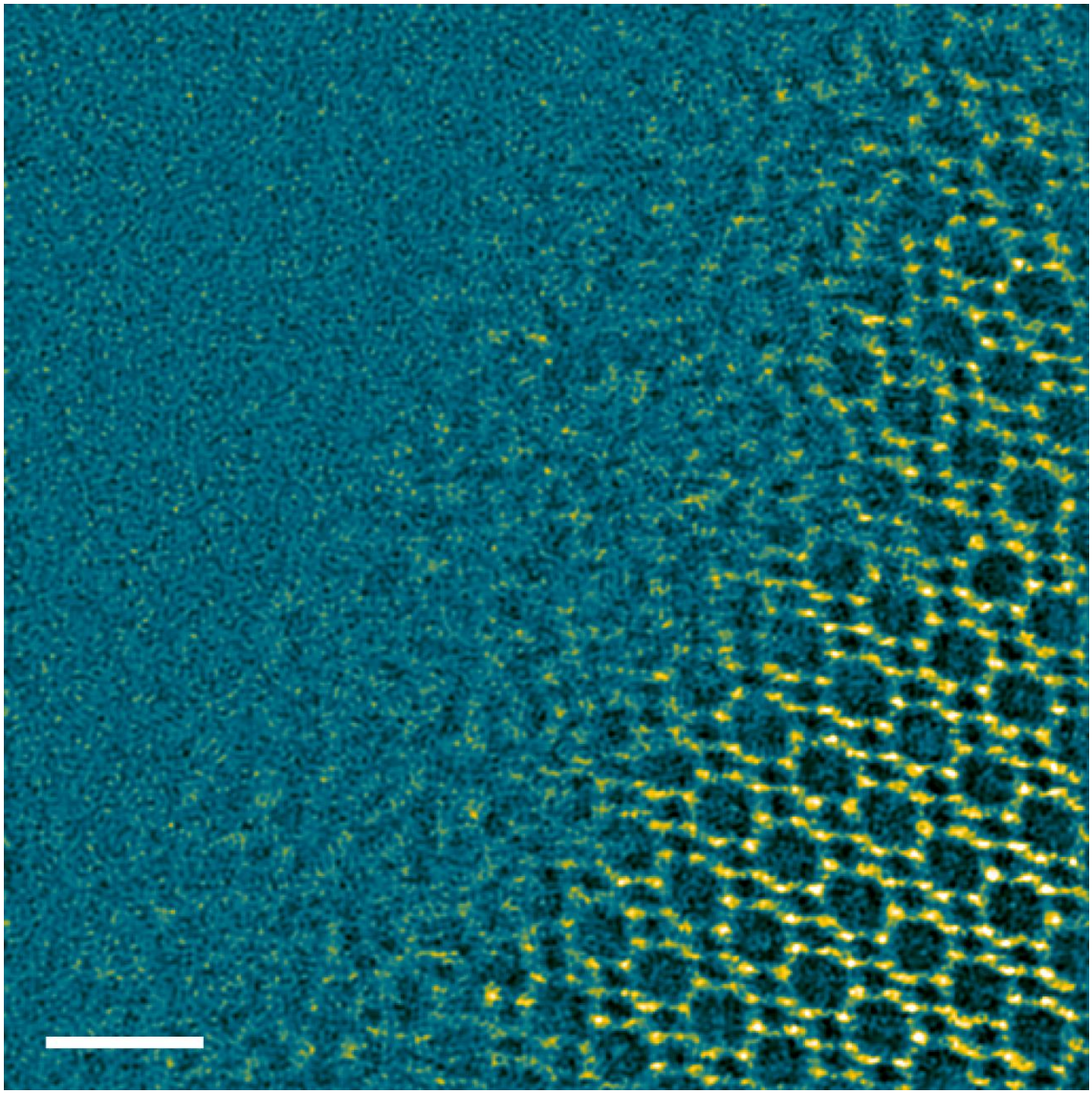

Figure S7

Electron ptychography image of H-SSZ-13 viewed along the [100] direction. Scale bar: 2 nm. The measured defocus of the recovered probe aberration is –1.9 nm.

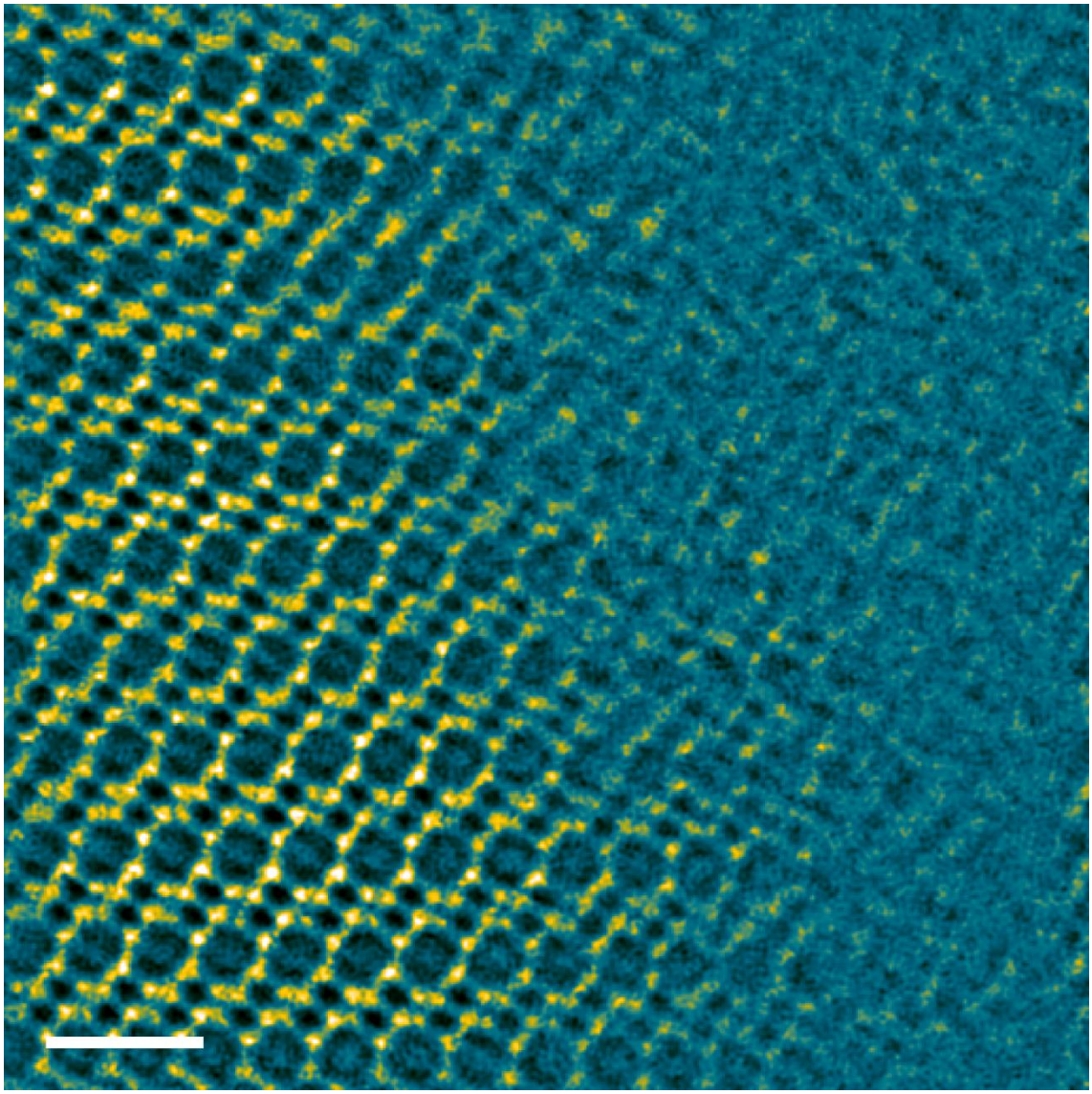

Figure S8

Electron ptychography image of Cu-SSZ-13 viewed along the [100] direction. Scale bar: 2 nm. The measured defocus of the recovered probe aberration is –1.4 nm (Figure S12).

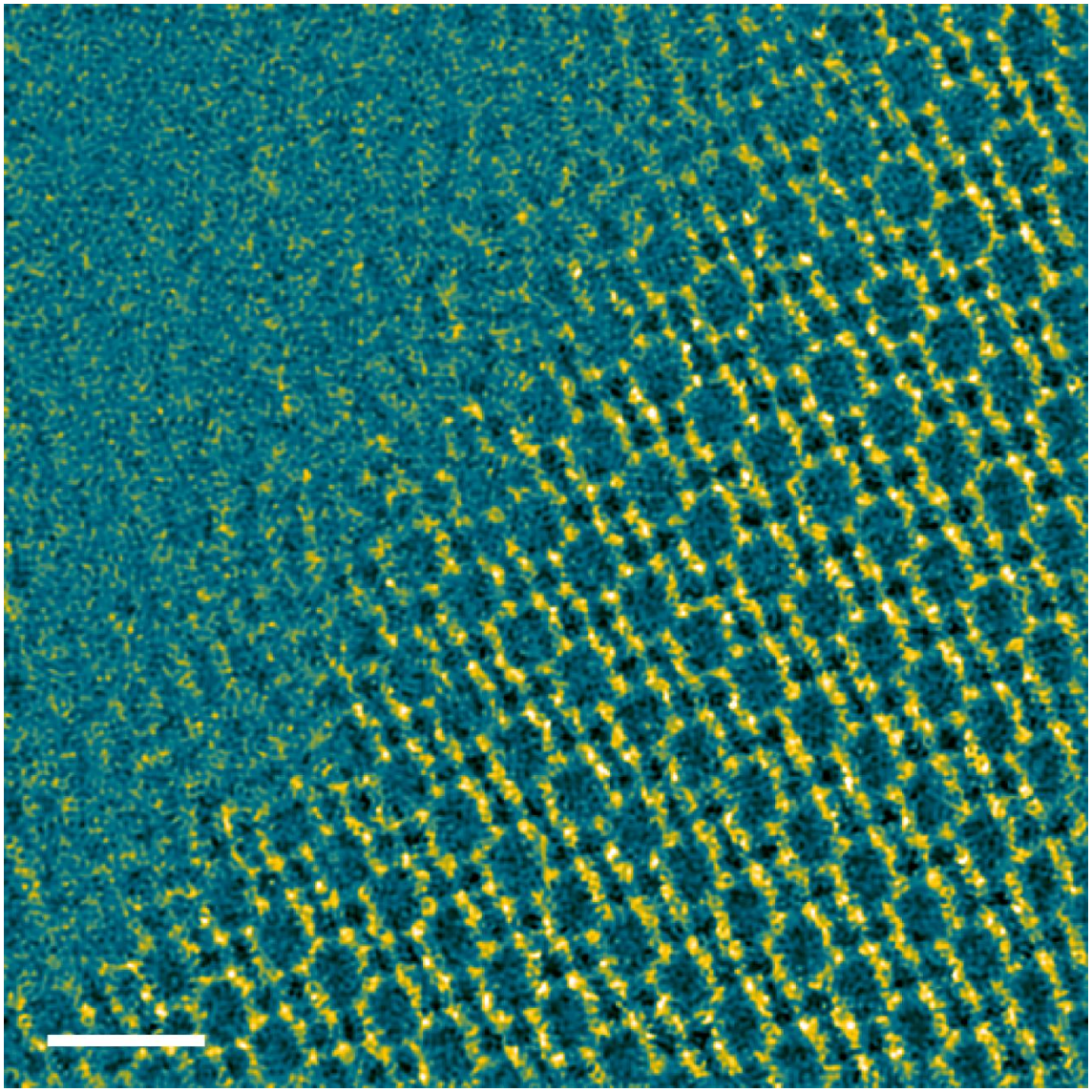

Figure S9

Electron ptychography image of Cu-SSZ-13-HTA viewed along the [100] direction. Scale bar: 2 nm. The measured defocus of the recovered probe aberration is 1.4 nm.

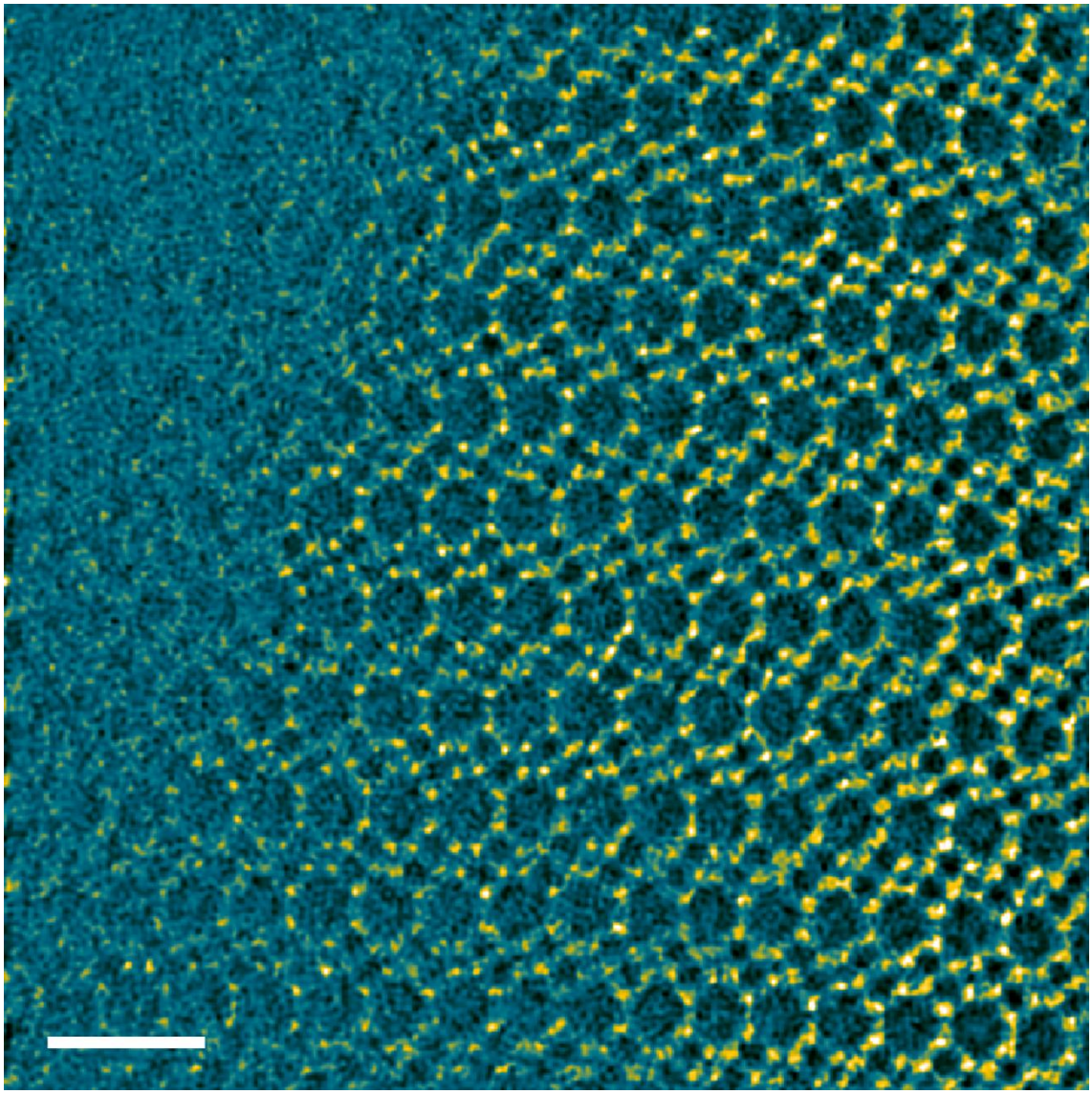

Figure S10

Electron ptychography image of Cu-SSZ-39 viewed along the [100] direction. Scale bar: 2 nm. The measured defocus of the recovered probe aberration is 1.4 nm (Figure S13).

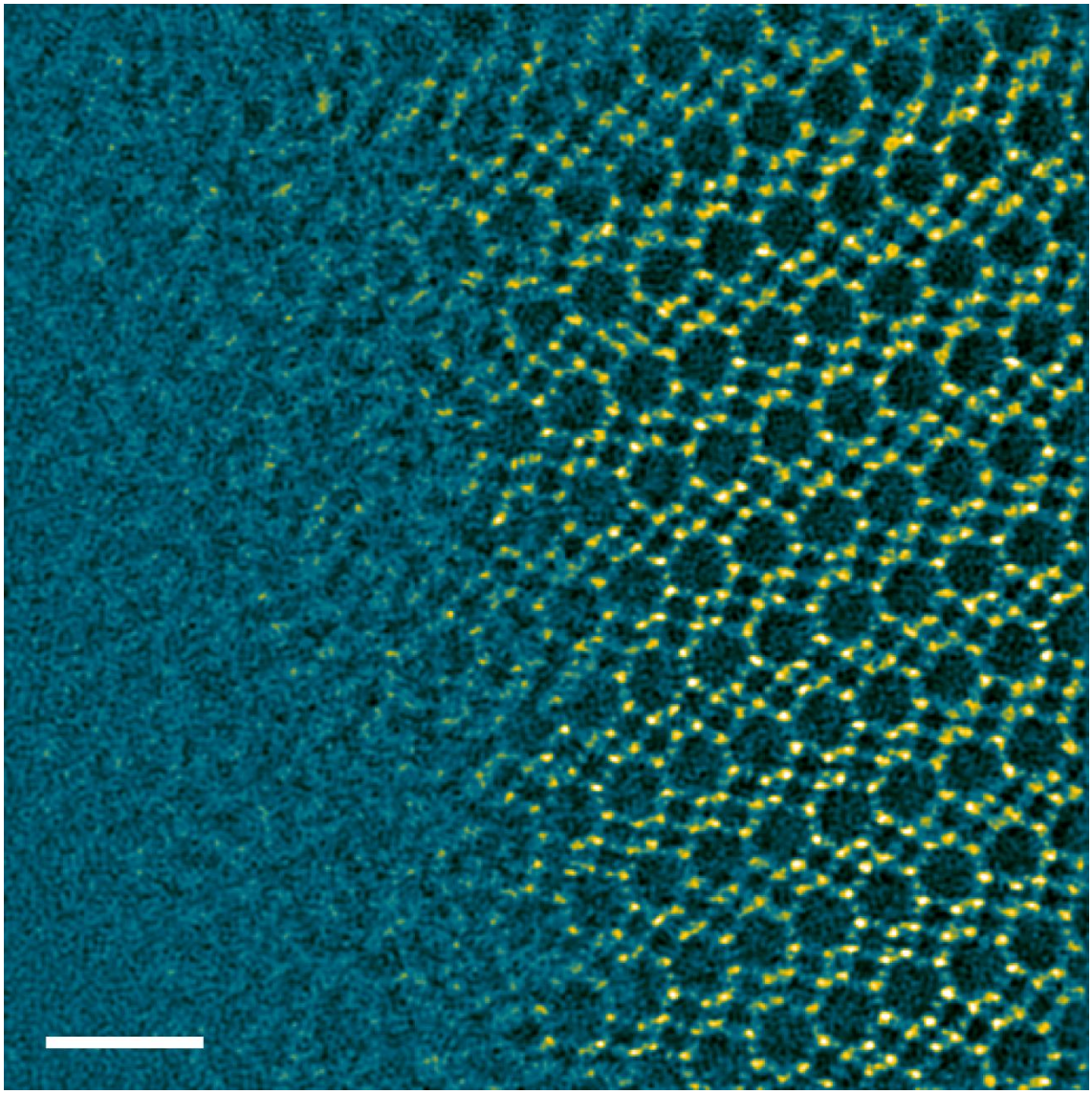

Figure S11

Electron ptychography image of Cu-SSZ-39-HTA viewed along the [100] direction. Scale bar: 2 nm. The measured defocus of the recovered probe aberration is –1.9 nm.

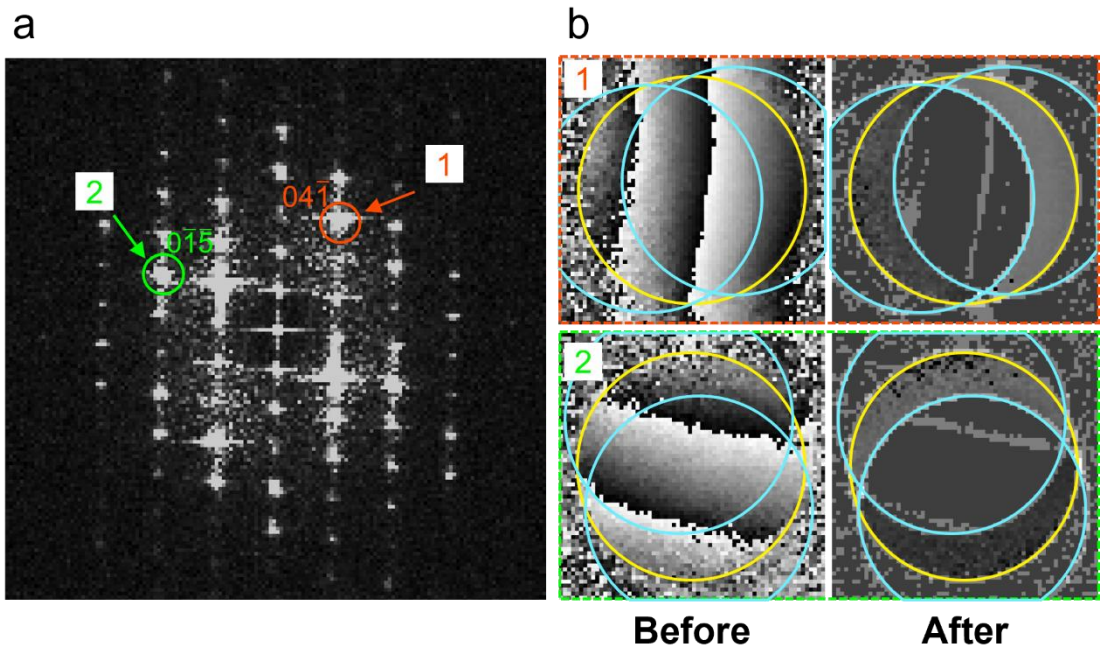

Figure S12

(a) Intensity maps of each Fourier component of a four-dimensional dataset, obtained by performing a Fourier transform with respect to the electron probe position. In the resulting map corresponding to the diffraction pattern, each pixel corresponds to a two-dimensional Fourier component. (b) The phases of the Fourier components at the positions corresponding to the $04\bar{1}$ (Position 1) and $0\bar{1}\bar{5}$ (Position 2) reflections indicated in (a) are shown before and after correction. The circles represent the positions of the transmitted wave disk (yellow) and the diffraction wave disks (sky blue) resulting from the $04\bar{1}$ and $0\bar{1}\bar{5}$ reflections. Before correction, the phase inclination due to defocus appears as a stripe pattern. Aberration correction by ptychography removes this phase inclination, as evidenced by the resulting uniform phase.

Note:

The measured defocus of the recovered probe aberration is –1.4 nm, which is less than 5 nm in absolute value, fulfilling the criteria for reliably evaluating the presence of Cu ions.

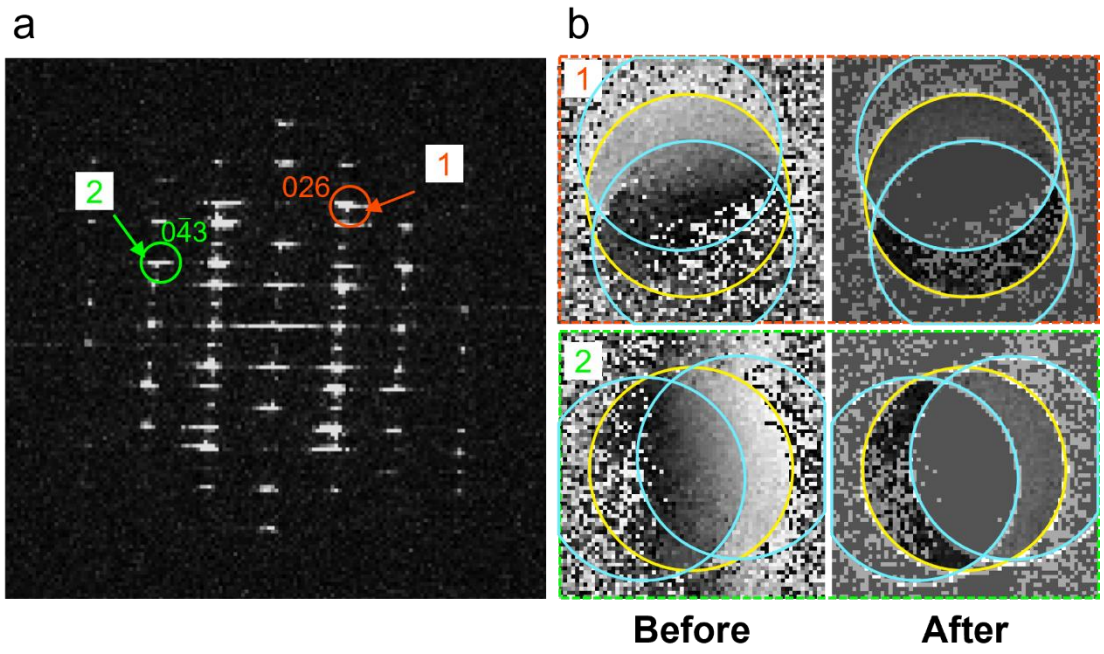

Figure S13

(a) Intensity maps of each Fourier component of a four-dimensional dataset, obtained by performing a Fourier transform with respect to the electron probe position. In the resulting map corresponding to the diffraction pattern, each pixel corresponds to a two-dimensional Fourier component. (b) The phases of the Fourier components at the positions corresponding to the 026 (Position 1) and 0$\bar{4}$3 (Position 2) reflections indicated in (a) are shown before and after correction. The circles represent the positions of the transmitted wave disk (yellow) and the diffraction wave disks (sky blue) resulting from the 026 and 0$\bar{4}$3 reflections. Before correction, the phase inclination due to defocus appears as a stripe pattern. Aberration correction by ptychography removes this phase inclination, as evidenced by the resulting uniform phase.

Note:

The measured defocus of the recovered probe aberration is 1.4 nm, which is less than 5 nm in absolute value, fulfilling the criteria for reliably evaluating the presence of Cu ions.

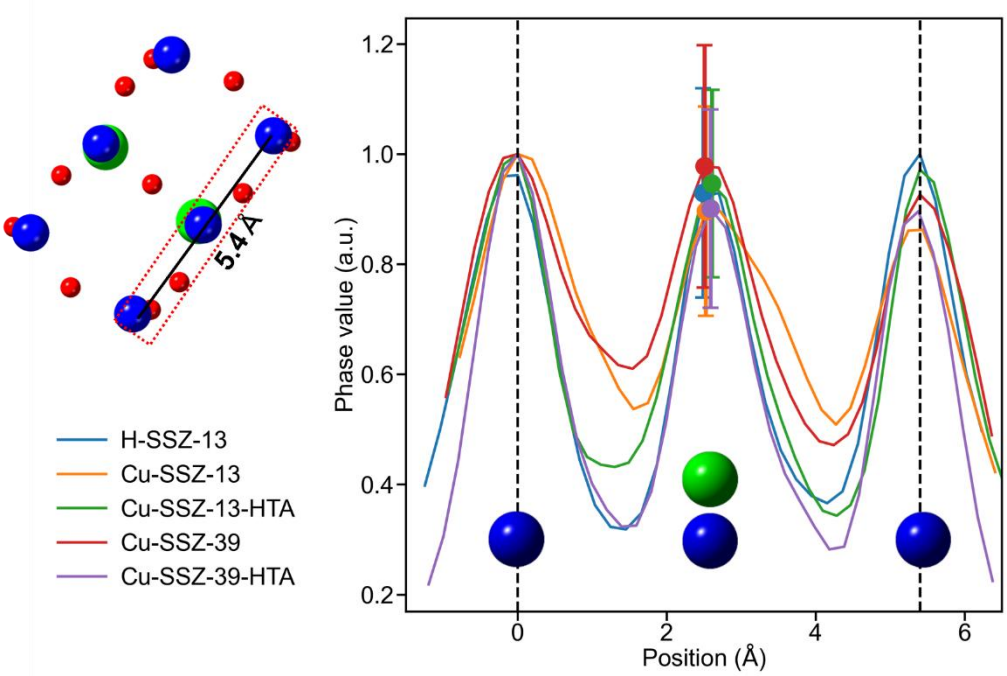

Figure S14

Line profiles across the double six-membered ring (d6r) site extracted from ptychographic phase images of H-SSZ-13 as well as of Cu-SSZ-13 and Cu-SSZ-39 before and after hydrothermal aging (HTA). The left inset shows the d6r unit and representative Cu sites.[4] The line profiles were obtained for the region between the Si atomic columns delineated by the red box. The vertical axis was normalized using the Si atomic columns at both ends of each profile. The error bars in the line profiles represent the standard deviation of the phase values measured at the central atomic column. These statistics were calculated using approximately 40 different d6r units extracted from the original ptychographic images (Figure S7–S11).

Note:

A comparison of the d6r site contrast across five samples showed that the d6r sites are superimposed on Si (Al) columns in projection from the [100] direction, making it impracticable to assess the presence or relative quantity of Cu ions from image contrast alone. Moreover, there is no alternative zone axis in Cu-SSZ-39 that can make the d6r units align with the incident electron beam. Accordingly, it is difficult to evaluate the Cu ion content at d6r sites via two-dimensional projection images, making it challenging to compare the Cu ion contents at the d6r sites for the two zeolites.

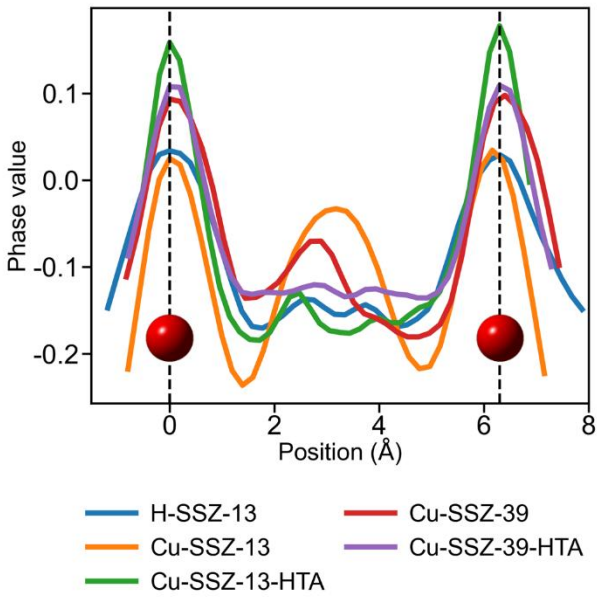

Figure S15

Line profiles across the eight-membered ring (8mr) region between O atomic columns, obtained from ptychographic phase images of H-SSZ-13 as well as of Cu-SSZ-13 and Cu-SSZ-39 before and after hydrothermal aging (HTA). The profiles are not normalized, and the vertical axis shows the measured phase values. The phase in the vacuum region is zero.

Table S1

The full width at half maximum (FWHM) of each peak in the X-ray diffraction (XRD) patterns of Cu-SSZ-13 and Cu-SSZ-39 obtained before and after hydrothermal aging (HTA) shown in Figure S2

Peak	Cu-SSZ-13 (deg)	Cu-SSZ-13-HTA (deg)	Cu-SSZ-39 (deg)	Cu-SSZ39-HTA (deg)
1	0.15	0.13	0.15	0.15
2	0.15	0.16	0.17	0.17
3	0.17	0.18	0.29	0.24

1 K. Mitsuishi, K. Nakazawa, R. Sagawa, M. Shimizu, H. Matsumoto, H. Shima and T. Takewaki, *Sci Rep*, 2023, **13**, 316.
2 J. Rodenburg and R. Bates, *Philosophical Transactions of the Royal Society of London. Series A: Physical and Engineering Sciences*, 1992, **339**, 521–553.
3 H. Yang, R. N. Rutte, L. Jones, M. Simson, R. Sagawa, H. Ryll, M. Huth, T. J. Pennycook, M. L. H. Green, H. Soltau, Y. Kondo, B. G. Davis and P. D. Nellist, *Nat Commun*, 2016, **7**, 12532.
4 A. M. Beale, I. Lezcano-Gonzalez, W. A. Slawinksi and D. S. Wragg, *Chem. Commun.*, 2016, **52**, 6170–6173.